© 2014. Published by The Company of Biologists Ltd | The Journal of Experimental Biology (2014) 217, 4328-4336 doi:10.1242/jeb.111773

RESEARCH ARTICLE

Prey fish escape by sensing the bow wave of a predator

William J. Stewart[1], Arjun Nair[1], Houshuo Jiang[2] and Matthew J. McHenry[1,*]

ABSTRACT

Prey fish possess a remarkable ability to sense and evade an attack from a larger fish. Despite the importance of these events to the biology of fishes, it remains unclear how sensory cues stimulate an effective evasive maneuver. Here, we show that larval zebrafish (*Danio rerio*) evade predators using an escape response that is stimulated by the water flow generated by an approaching predator. Measurements of the high-speed responses of larvae in the dark to a robotic predator suggest that larvae respond to the subtle flows in front of the predator using the lateral line system. This flow, known as the bow wave, was visualized and modeled with computational fluid dynamics. According to the predictions of the model, larvae direct their escape away from the side of their body exposed to more rapid flow. This suggests that prey fish use a flow reflex that enables predator evasion by generating a directed maneuver at high speed. These findings demonstrate a sensory-motor mechanism that underlies a behavior that is crucial to the ecology and evolution of fishes.

KEY WORDS: Biomechanics, Lateral line, Flow sensing, Predation, Particle image velocimetry, Computational flow dynamics

INTRODUCTION

Predation is fundamental to the biology of fish predators and prey. From the earliest stages of growth, prey fish survive attacks by fish predators with the 'fast-start' escape response (Fuiman and Magurran, 1994). Although this maneuver displaces a larval fish by less than a body length (Kimmel et al., 1974), it is effective because of limitations inherent to the predatory strike. Predator fish commonly use suction feeding, where the prey is targeted by low pressure created through the rapid expansion of the mouth cavity. This is effective over a small region directly in front of the mouth for a brief period (Kimmel et al., 1974; Day et al., 2007). Therefore, prey survive by escaping just beyond the limited reach of a predator.

It is unclear how the sensory systems of prey fish operate quickly enough to coordinate an evasive maneuver. The visual system can recognize a predator at a distance (Dill, 1974), but requires substantial neuronal processing that can delay an escape. For example, it takes most zebrafish (*Danio rerio*) larvae at least 200 ms to react to a visual stimulus (Burgess and Granato, 2007), which is about an order of magnitude longer than the duration of mouth opening during suction feeding (Wainwright et al., 2001; Day et al., 2007). In contrast, prey fish can respond to a flow stimulus in less than 4 ms (Liu and Fetcho, 1999) and thereby escape before the predator opens its jaws (Stewart et al., 2013). Flow sensing is achieved by the lateral line system, which includes mechanoreceptors with hair cells in the skin (Dijkgraaf, 1963). An experimental ablation of these cells causes larval fish to fail to survive predatory attacks, even when the visual system is unimpaired (Stewart et al., 2013). Therefore, the lateral line is necessary for survival, but it remains unclear what role flow sensing plays in coordinating an escape.

Here, we present results that demonstrate how predator evasion is facilitated by the lateral line system. This was determined by behavioral experiments that exposed larval zebrafish in the dark to the controlled flow generated by a predator robot. This flow, known as the bow wave (Holzman and Wainwright, 2009), was measured by flow visualization and modeled with computational fluid dynamics. We examined the three-dimensional high-speed responses of larvae in relation to the bow wave. Furthermore, we compared our observed fast-start responses with the results of several behavioral algorithms that mathematically predicted the direction of fast starts. The results of these approaches suggest that prey survive by evading the predator with a directed reflex that is stimulated by the bow wave.

RESULTS

Robotic predator

We exposed larval fish to the flow generated by the motion of a robotic predator. This robot consisted of a motor-driven translation stage that propelled the body of a dead adult zebrafish through the center of a water-filled tank that contained zebrafish larvae in the dark (see the Materials and methods for details). Using infrared illumination, two video cameras recorded the behavioral responses of larvae that were not mediated by vision. Under these conditions, we found the robot provided a mimic of the predator that was sufficient to consistently stimulate a fast start. All larvae along the predator's path (N=202) responded within 2 cm to the predator's approach with a fast start (Fig. 1; supplementary material Movie 1). The approach speed of the predator significantly affected the response distance of the prey (Fig. 2; one-way ANOVA, d.f.=2, N=198, P<<0.01), with larvae approached at high speed (20 cm s^{-1}) responding from slightly greater distances than larvae approached at 2 or 11 cm s^{-1} (Tukey–Kramer multiple comparison method for unequal sample sizes, P<0.05) (Dunnett, 1980).

The vast majority of fast-start responses were directed away from the robotic predator. We found that the fast start increased distance from the initial position of the predator in 96% of larvae (N=202). Larvae positioned to the side of the predator robot generally moved laterally, irrespective of approach speed. This was indicated by larvae positioned at least 0.5 cm lateral to the body axis of the predator exhibiting a median azimuth (±1 median deviation) of 59.2±48.8 deg (N=14), 69.2±30.6 deg (N=16) and 47.5±35.8 deg (N=20), respectively, for approach speeds of 2, 11 and 20 cm s^{-1} (Fig. 1C). Similarly, larvae positioned ventral to the predator directed the fast start downward, irrespective of the predator's approach speed (Fig. 1D). Therefore, responses were directed in both azimuth and elevation. Larvae positioned directly in front of (Fig. 1C), or dorsal to (Fig. 1D), the predator swam away in a variety of directions.

[1]Department of Ecology and Evolutionary Biology, University of California, Irvine, CA 92697-2525, USA. [2]Department of Applied Ocean Physics and Engineering, Woods Hole Oceanographic Institution, Woods Hole, MA 02543-1050, USA.

*Author for correspondence (mmchenry@uci.edu)

Received 30 July 2014; Accepted 27 October 2014

The Journal of Experimental Biology

The Journal of Experimental Biology (2014) doi:10.1242/jeb.111773

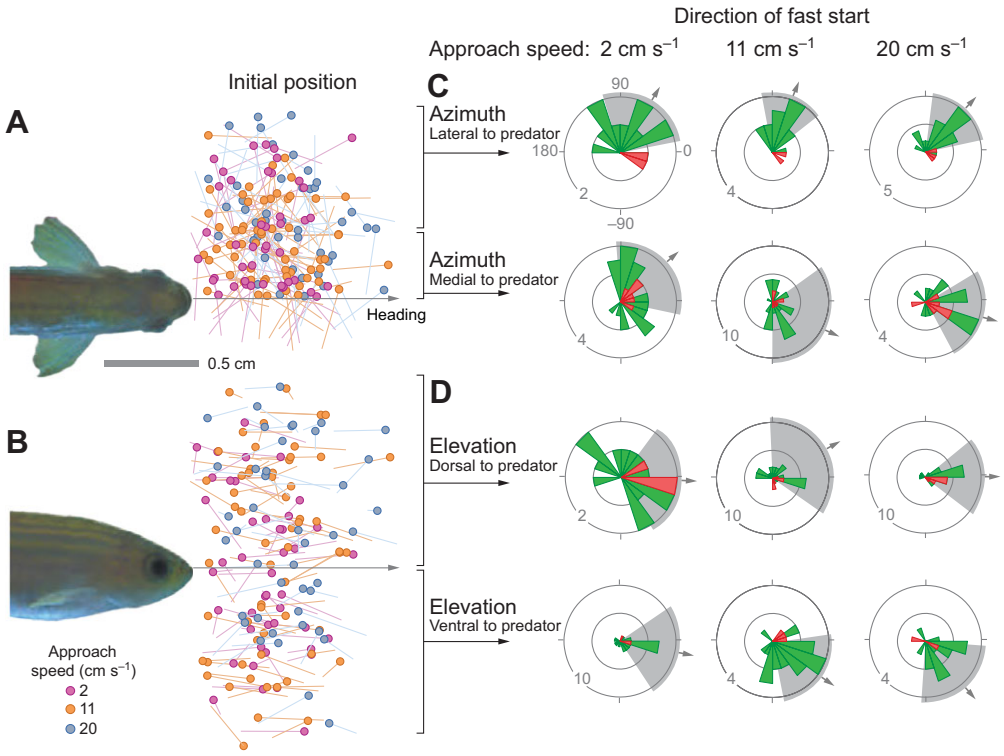

Fig. 1. The position and direction of the fast start in response to a robotic predator in zebrafish (*Danio rerio*). (A,B) Each filled circle indicates the position of the prey's rostrum and the line extends to the end of the tail where a fast start was initiated. Positions are indicated from dorsal (A) and lateral (B) views. (C,D) The direction of the fast start was measured by its azimuth (C) and elevation (D) angles with respect to the predator's heading for each approach speed (columns) and position (rows). Responses were scored by motion away (in green) or toward (in red) the predator's heading with median direction (arrow) and mean deviation (gray area).

The lateral line system was manipulated to determine whether these responses were mediated by flow sensing. We found that larvae with a compromised lateral line system failed to respond to an encounter with our robot. In particular, 30 larvae positioned directly on the path of the robot's motion were swept aside without exhibiting any swimming in response (e.g. supplementary material Movie 2). This suggests that the fast start of untreated fish (Fig. 1) was mediated by the lateral line system.

Computational fluid dynamics

We developed a computational fluid dynamics (CFD) model of the flow generated by the predator's motion (Fig. 3A) to understand the flow stimulus to which larvae were exposed in our behavioral experiments. We tested this model by comparing its flow field predictions against flow visualization measurements by particle image velocimetry (PIV). Because of limitations in the sensitivity of the PIV measurements, we focused this comparison on regions in the flow field that exceeded 0.5 cm s^{-1} in the bow wave and where larvae responded to the predator (Fig. 1). We found that the PIV and CFD flow fields agreed in the qualitative spatial pattern of flow (Fig. 3B) and that the values for flow speed were similar. The average difference between the PIV and CFD speeds at each position was less than 7% for all approach speeds. Therefore, there was good agreement between the model and flow visualization.

Our examination of the bow wave predicted by CFD found that flow speed was roughly proportional to the speed of a predator's approach. Therefore, the ratio of flow speed to approach speed was similar for all approaches (Fig. 3E) with a spatial pattern characterized by rapid attenuation of speed with distance ahead of the predator. To examine the dependency of the bow wave on Reynolds number, we conducted simulations with an ideal (i.e. inviscid) fluid. This condition yielded a wake behind the body that contrasted what was predicted for realistic Reynolds numbers due to viscous effects (Fig. 3C,D). Despite this difference, the bow wave flow was largely similar (Fig. 3E). The only substantial deviation between viscous and inviscid simulations was apparent within 2 mm of the predator's rostrum, where the boundary layer influences the profile of the bow wave. Larvae rarely responded to flow in this close proximity (Fig. 1). Therefore, the bow wave flow field is largely independent of Reynolds number for the range of values presently considered (*Re*>450).

We combined the results of CFD simulations and our behavioral experiments to consider how larvae use spatial cues in the bow wave to direct a fast start. The azimuth angle of the mean flow velocity along the length of a larval body was not found to be significantly correlated with the azimuth of the fast start (Fig. 4, P=0.29, N=203). Therefore, larvae did not align their response with respect to flow velocity. However, we did find that larvae consistently directed their fast start away from rapid flow when we transformed the flow field

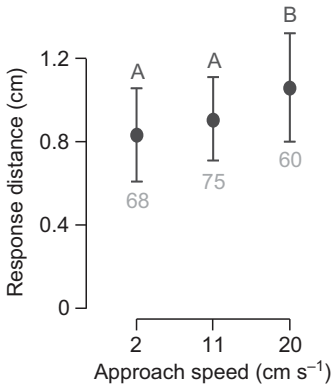

Fig. 2. The response distance of prey. The distance separating the rostrum of the predator and closest position of the prey body at the time of prey response for varying approach speed (mean ± 1 s.d.) with numerical values indicating sample size. Prey approached at 20 cm s^{-1} responded from a greater mean distance than prey approached at slower speeds (one-way ANOVA, d.f.=2, N=198, P<<0.01; Tukey–Kramer multiple comparison method for unequal sample sizes, P<0.05).

The Journal of Experimental Biology (2014) doi:10.1242/jeb.111773

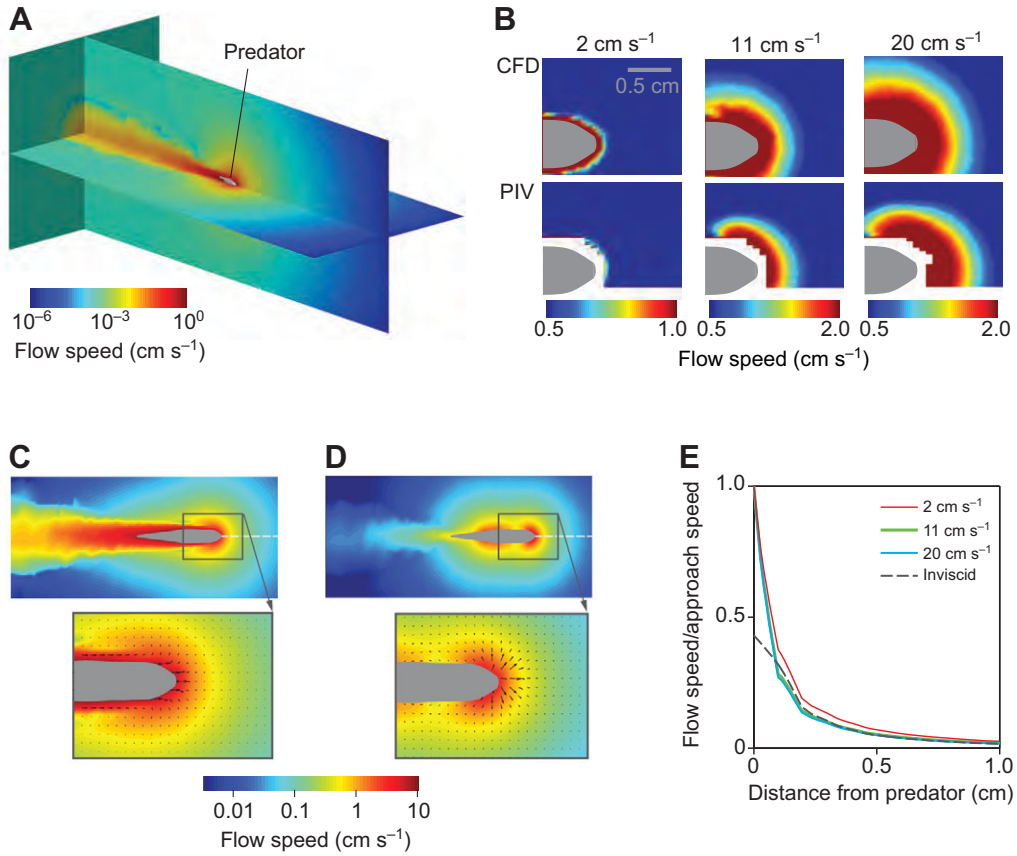

Fig. 3. The bow wave of a predator. A computational fluid dynamics (CFD) model was developed to determine the flow generated by our robotic predator. (A) The flow speed predicted by the model, visualized around the predator (in gray) for an approach speed of 11 cm s^{-1}. (B) A dorsal view of the predator's head and the flow speed for the mid-frontal plane predicted by CFD (top row) and verified by flow visualization by particle image velocimetry (PIV) (bottom row) for the three approach speeds. Flow speed at the surface of the predator was anticipated to match the approach speed (as in E), but the scaling of the colormap was set at a lower maximum to emphasize the spatial variation in the regions where larvae responded. (C,D) CFD simulations that both included (C) and excluded (D) viscosity for an approach speed of 11 cm s^{-1}. As in B, the flow is shown from the dorsal view, with a detail of the flow velocity of the bow wave overlaid as vectors for a region anterior to the predator. (E) The ratio of flow speed to approach speed is plotted as a function of distance from the predator along a line directly in front of the predator (dashed white line in C and D). These values included a consideration of viscous forces for a range of Reynolds numbers (Re) that were generated by varying the approach speed (Re=450 for 2 cm s^{-1}, Re=2500 for 11 cm s^{-1} and Re=4500 for 20 cm s^{-1}). Inviscid simulations predicted equivalent normalized values for flow at all approach speeds. For positions beyond 0.2 cm, the ratio of flow speed to approach speed was shown to be highly similar for all cases.

with respect to the larva's local frame of reference (Fig. 5A,B). By this transformation, all positive azimuth angles indicated responses away from the side of the body exposed to flow of higher velocity for approach speeds of 2 cm s^{-1} (109.0±55.8 deg, N=45), 11 cm s^{-1} (98.7±54.7 deg, N=60) and 20 cm s^{-1} (87.8±36.6 deg, N=44). These values indicate that the median response was directed at an approximate right angle in azimuth with respect to the initial orientation of the body for the approach for the two faster approach speeds (Fig. 5C). The consistency of this response occurred despite large differences in the flow encountered by larvae in different positions and orientations. A more subtle directional response was measured in elevation. Larvae did not direct responses in elevation when the ventral surface of the body was exposed to more rapid flow (Fig. 6A). However, more rapid flow on the dorsal surface directed responses slightly downwards (Fig. 6B) for approach speeds of 2 cm s^{-1} (−11.2±15.2 deg, N=25), 11 cm s^{-1} (−14.1±20.9 deg, N=28) and 20 cm s^{-1} (−24.0±20.7 deg, N=18).

Behavioral algorithm modeling

We tested whether our measurements were consistent with the predictions of particular behavioral algorithms. Predictions were determined for each measured position and orientation for the bodies of larvae that responded to the robotic predator (Fig. 1A,B). We modeled the flow reflex as a response directed normal to the initial orientation of the body, away from the side of the body exposed to the faster maximum flow speed (Fig. 7B). This algorithm predicted responses that were statistically indistinguishable (P>0.05, N=117 for medial, N=76 for lateral positions) from our measurements, according to the non-parametric Kuiper test (Batschelet, 1981). Another algorithm found to be indistinguishable from our measurements also directed the fast start away from the side of the body exposed to rapid flow, but at a random angle with respect to the initial body orientation (Fig. 7C). In contrast, we found highly significant differences (P≤0.001) when the response was directed toward the side of the body exposed to rapid flow and a right angle (Fig. 7D) or in a completely random direction (Fig. 7E).

DISCUSSION

Our results suggest that prey fish evade predators by executing a directed fast start in response to the flow generated by the predator. These responses appear to be mediated by the lateral line because compromising this system in our experiments extinguished

The Journal of Experimental Biology (2014) doi:10.1242/jeb.111773

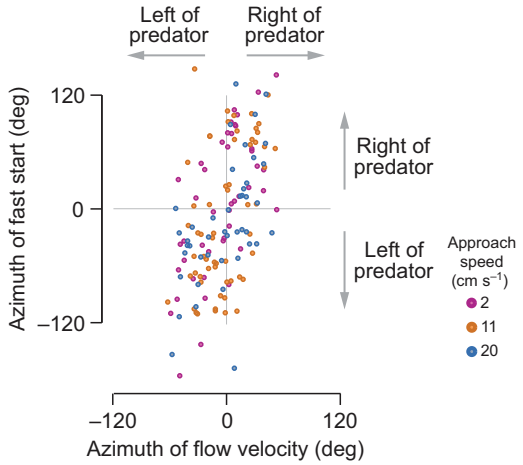

Fig. 4. The azimuth angle of flow velocity and fast-start direction. A scatterplot of the azimuth of the fast start direction with respect to the azimuth of the flow velocity (determined by CFD at the position of each larva). These were defined with respect to the predator, such that an azimuth of 90 deg is perpendicular to the predator's heading (Fig. 1). These variables are not significantly correlated (P=0.29, N=203).

responses to a robotic predator's approach. In addition, the direction of the fast start (Fig. 1) was oriented away from high flow (Figs 5, 6) in a pattern that was consistent with responses to flow stimuli. These results support earlier findings that flow sensing plays a major role in the survival of larval zebrafish prey (Stewart et al., 2013) and offers a basis for understanding a sensory-motor mechanism of predator evasion.

Directional responses

The direction of a fast start can influence its effectiveness in predator evasion. We found that larvae moved away from a predator's heading most successfully when positioned lateral (Fig. 1A,C) and ventral (Fig. 1B,D) to the predator. These responses are consistent with optimal evasion strategies predicted by differential game theory modeling (Isaacs, 1965). A previous application of this theory to fish demonstrated how prey that move much faster or much slower than a predator should execute a fast start at a right angle from the predator's heading to maximally increase their distance from the predator (Weihs and Webb, 1984). Consistent with this prediction, we found that larvae positioned lateral to the predator moved in a lateral direction (Fig. 1C). However, larvae also exhibited a wide range of responses, most of which were not clustered around this optimum. It is therefore possible that the flow created by a slow approach presents a relatively weak directional signal that fails to accurately inform the prey about the predator's heading.

Faster approach speeds by the robotic predator elicited responses that were more consistent with optimal strategy (Fig. 1C), which predicts that the azimuth angle decreases with approach speed (Weihs and Webb, 1984). In addition, larvae exposed to the two faster approaches moved with elevation angles that were more directed downwards than the slow approach (Fig. 1D). Therefore, larvae more effectively moved to evade the robotic predator when approached at a faster speed. This result may be due to a more intense lateral line stimulus generated by a faster approach (Fig. 3). According to this argument, faster flow serves to more effectively alert a prey to the predator's heading and thereby stimulates a consistently directed response. However, these patterns did not emerge for larvae positioned dorsal to (Fig. 1D), and in front of (Fig. 1C), the approaching predator.

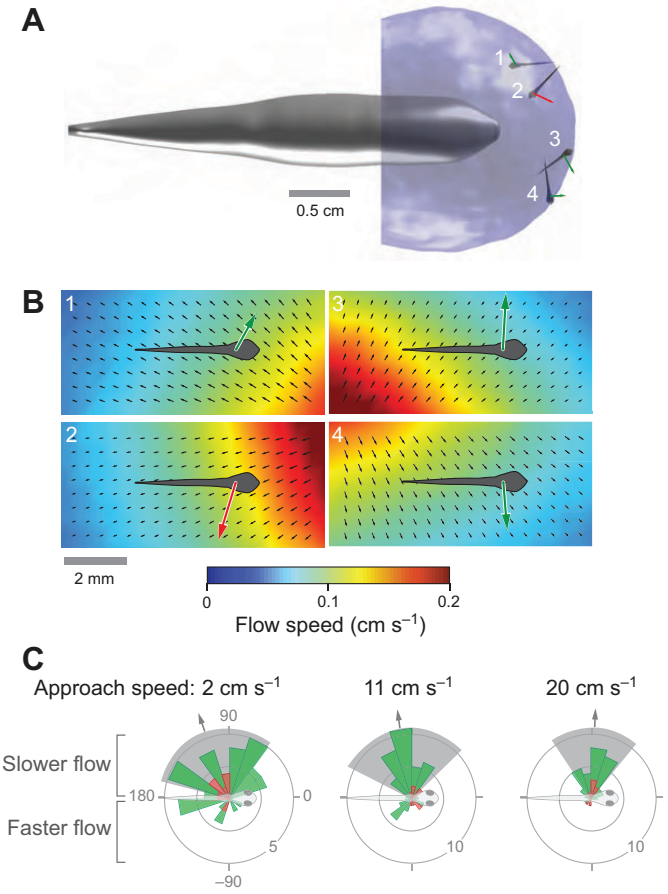

Fig. 5. The direction of flow and the fast start with respect to a larva's body. (A) An isosurface of the flow speed (0.1 cm s^{-1}) illustrates the 3D shape of the bow wave. This flow field was transformed into the local frame of reference for individual larvae. This transformation is illustrated for four representative individuals (1–4), which are shown at their initial position with respect to the predator robot (as in Fig. 1A). The measured direction and displacement of the fast start is indicated for each response, which moved larvae toward (in red) or away (in green) from the predator's heading. (B) The velocity of flow and fast-start direction are shown in the local frame of reference prior to the initiation of the fast start, along the mid-frontal plane of each larva (1–4) in A. In this frame of reference, we evaluated whether the mean flow speed was greater on the left or right side of the body. (C) The direction of the fast start (in azimuth) is shown with respect to the side of the body exposed to a greater flow speed. As in Fig. 1, responses were scored by motion away (in green) or toward (in red) the predator's heading with median direction (gray arrow) and mean deviation (gray area).

Despite these consistencies with optimal strategy, our measurements do indicate some strategic limitations. Escape responses are most effective when unpredictable (Humphries and Driver, 1970; Weihs and Webb, 1984; Domenici et al., 2011) whereas we found the responses of larvae positioned lateral to a fast approaching predator to be consistent and therefore predictable (Fig. 1C). Furthermore, prey positioned in front of the predator consistently moved in the direction of a fast-approaching predator, where the predator might more easily overtake them (Fig. 1C,D).

The bow wave

Our results are consistent with idea that prey evade predators by initiating an escape in response to the flow generated by a predator's approach (Viitasalo et al., 1998; Kiørboe and Visser, 1999; Visser, 2001; Heuch et al., 2007; Casas et al., 2008; Holzman and Wainwright, 2009; Gemmell et al., 2014; Seamone et al., 2014).

The Journal of Experimental Biology (2014) doi:10.1242/jeb.111773

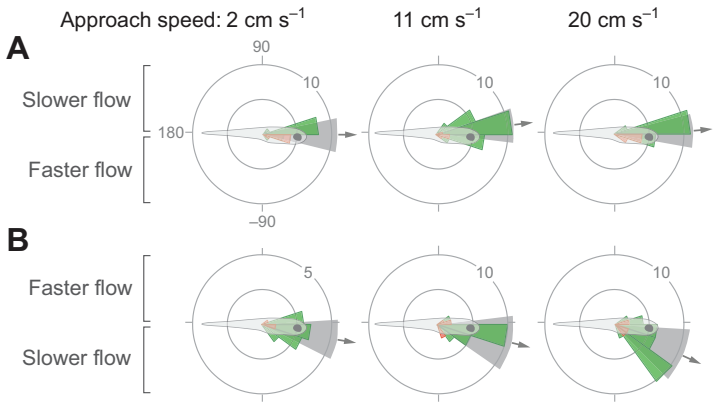

Fig. 6. The elevation of the fast start. The fast-start direction was transformed into the larva's frame of reference prior to motion and displayed in the same manner as the azimuth angles in Fig. 5C. Responses were separated according to whether larvae were exposed to more rapid flow on (A) the ventral surface or (B) the dorsal surface of the body, as determined by CFD.

This flow field is commonly referred to as a 'bow wave', although it does not exhibit the oscillations that are typical of a wave and it is a distinct phenomenon from the surface waves of the same name. The submerged body of a predator does not produce the gravitational surface waves generated by a ship, but rather creates a flow disturbance as it moves forward (Fig. 3). In addition, the flow generated by a predator does not propagate freely like a wave, but instead dissipates quickly after the predator stops moving. Despite these potential complications, we know of no better term than 'bow wave' and therefore presently adopt this phrase.

We examined the bow wave for differences due to the Reynolds number of the predator. When normalized by approach speed, the flow velocity of the bow wave exhibited a similar monotonic decay with distance (Fig. 3E). Furthermore, a simulation with an inviscid fluid exhibited the same general pattern, despite differences in the wake posterior to the predator's body (Fig. 3C,D). The main discrepancy in the bow wave between viscous versus inviscid simulations was apparent within a millimeter of the predator's rostrum, where the viscous boundary layer was apparent. However, we found that the vast majority of prey responded to the bow wave outside this region (Fig. 1B), which suggests that the relevant stimuli may be attributed to a phenomenon that is essentially independent of the predator's Reynolds number. The bow wave therefore could be represented by a potential flow model that is easier to implement than the CFD model that we developed.

The flow reflex

We used the results of our CFD simulations to examine the flow conditions that succeeded in stimulating a fast start in prey fish. By the end of the fast start (i.e. completion of stage 2), larvae traversed about 90 deg from their starting orientation (Fig. 5C). The azimuth of this ultimate direction did not correlate well with the azimuth of flow velocity (Fig. 4), but larvae consistently moved away from the side of the body exposed to faster flow. Therefore, the ability of larval fish to move away from the predator (Fig. 1) appears to be a consequence of deciding to move to the left or right at an angle that does not depend on the flow stimulus. We will refer to this behavior as the 'flow reflex' (Fig. 8), which is a behavior that is consistent with previous reports of the escape response stimulated in larval fish by water flow (Blaxter and Fuiman, 1989; Liu and Fetcho, 1999; McHenry et al., 2009). The binary directionality of this behavior may explain its strategic failures discussed above. Therefore, the

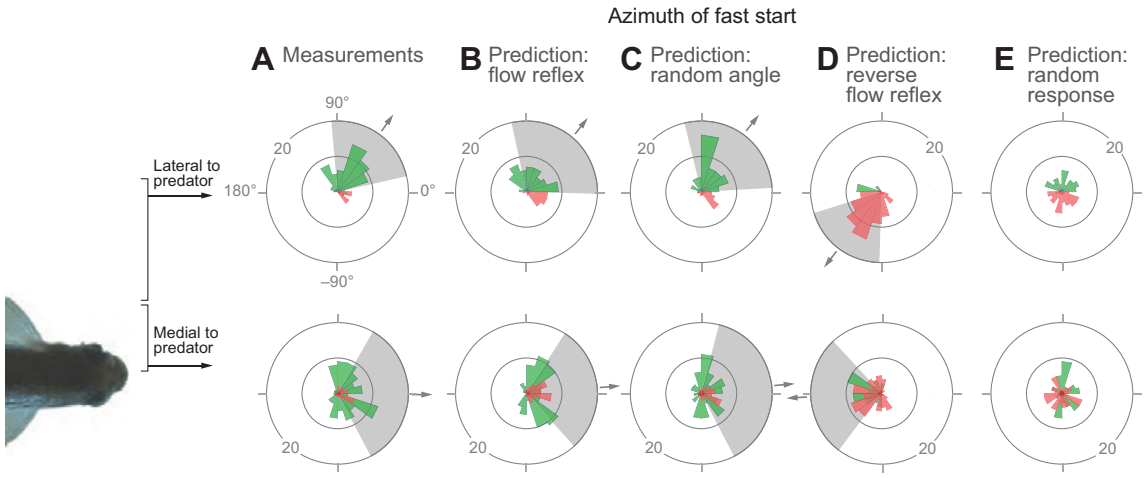

Fig. 7. Fast start direction predicted by behavioral algorithms. For each larva (Fig. 1A,B), measurements of the azimuth of the fast start were compared to the predictions by behavioral algorithms. (A) The measurements of azimuth were separated according to position medial (N=117) or lateral to (>0.5 cm, N=76) the predator for all approach speeds (i.e. all measurements in Fig. 1C). (B) The flow reflex was modeled by rotating the larva at a right angle from its initial orientation, away from the side of the body exposed to higher maximum flow speed. This algorithm showed directions that were statistically indistinguishable (P>>0.05) from our measurements in A [Kuiper test (Batschelet, 1981)]. (C) Predicted responses were also indistinguishable for an algorithm that produced responses directed at a random angle, but away from the side of the body exposed to faster flow. Significant deviation from measurements was observed (P=0.001) when we modeled larvae as moving toward the side of the body exposed to greater flow at a right angle (D) and toward a random side of the body at a random angle (E). As in Fig. 1, responses were scored by motion away (in green) or toward (in red) the predator's heading with median direction (arrow) and mean deviation (gray area).

The Journal of Experimental Biology (2014) doi:10.1242/jeb.111773

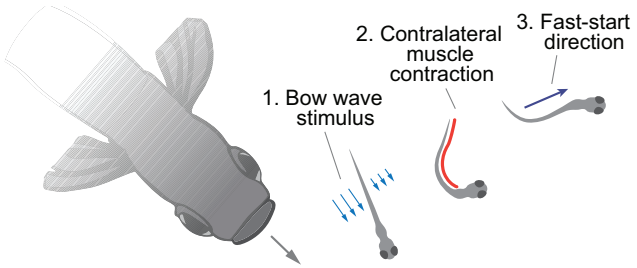

Fig. 8. Directional control of the fast start. A schematic illustration of the proposed flow reflex for a prey fish's response to a predator. (1) The predator's bow wave exposes the side of the prey's body closer to the predator to rapid flow. (2) This flow triggers the muscles on the contralateral side of the body to contract, which (3) directs the fast start away from the predator.

minimal sensory processing that facilitates the high-speed response might limit the ability of the flow reflex to direct an optimal escape.

We modeled behavioral algorithms to test whether our measurements agree with the flow reflex. In separate algorithms, the response direction was calculated at a right angle (Fig. 7B) or random angle (Fig. 7C) with respect to the body. Both models replicated the observed patterns of directional responses (Fig. 1A,C; Fig. 7A), but only when the responses were directed away from the side of the body exposed to rapid flow (Fig. 7D,E). Therefore, larvae move in a manner that is consistent with the flow reflex. However, responding at any particular angle with respect to the prey's body is not important in determining the overall direction of the response.

The flow reflex is consistent with our understanding of the neurophysiology of zebrafish larvae. Lateral line hair cells are innervated by a population of neurons that transmit encoded flow stimuli to command neurons for the escape circuit on the contralateral side of the body (Liao, 2014). This circuit accounts for the ability of flow on one side of the body to stimulate motion on the opposite side (Liu and Fetcho, 1999). Therefore, neurophysiological research on the escape circuit may aid our understanding of the mechanistic basis of predator–prey interactions.

In summary, the flow reflex offers a basis for understanding how interactions between predators and prey are mediated between fishes. It shows how a prey's survival depends on the hydrodynamics of flow stimuli, the sensitivity of the lateral line, the processing of flow cues by the nervous system and the motor control of the fast start. Future research in these areas of neuroscience and biomechanics will offer exciting perspectives for understanding what facilitates and constrains predator–prey interactions. These dynamics have the potential to play major roles in the ecology and evolution of a broad diversity of fishes.

MATERIALS AND METHODS

Animal husbandry

Zebrafish (*Danio rerio* Hamilton 1922) larvae served as the prey and adults as predators, as in previous experiments (Stewart et al., 2013). All zebrafish were bred from wild-type (AB line) colonies housed in a flow-through tank system (Aquatic Habitats, Apopka, FL, USA) that was maintained at 28.5°C on a 14 h:10 h light:dark cycle. The fertilized eggs from randomized mating were cultured according to standard techniques (Westerfield, 1993) and larvae were raised in an incubator in E3 embryo media (Brand et al., 2002). Only larvae that were 5 days post-fertilization were used in experiments, which included a total of 268 larvae (body length=0.40±0.038 cm, mean ± 1 s.d.).

Robotic predator experiments

A robot allowed us to replicate the hydrodynamics of a predator's approach toward prey fish with controlled motion (Fig. 9). The body of a formalin-fixed dead adult zebrafish served as the stimulus source, which was translated through the center of a water-filled tank (length×height×width=36×8×9 cm) that contained numerous larvae. The predator was held in place by a sting that was anchored to a sled that was free to glide along a rail system (high-speed 23 mm needle-roller carriages on 64 mm guide rails, McMaster-Carr, Santa Fe Springs, CA, USA) and was pushed by a magnetic-drive linear servo motor (model P01-23×160, LinMot Inc., Elkhorn, WI, USA) at constant speed. The sled additionally carried two high-speed video cameras (Photon Focus DR1, Norpix Inc., Montreal, CA, recording at 500 frames s^{-1} with 640×480 pixel resolution) that focused on the predator's head and region anterior to the predator (an area of 3.00×2.25 cm) from lateral (with the aid of a 45 deg mirror) and dorsal perspectives. The cameras recorded the motion of larvae contained within the tank as they encountered the robot. To remove the possibility of a visual response by larvae, experiments were performed in the dark under infrared (940 nm) illumination. This allowed larvae to be viewed using the IR-sensitivity of the cameras.

Larvae were acclimated to the tank prior to an experiment. We placed between 100 and 200 zebrafish larvae in the tank, which contained water held at 27°C. The preserved predator was positioned in the center of the tank at one end of the chamber. After a 20 min acclimation period, the predator was translated through the tank at one of three randomly selected approach speeds. The three speeds (2, 11 or 20 cm s^{-1}) spanned the range of measured values for adult zebrafish when preying on larval zebrafish (Stewart et al., 2013). This process was repeated after returning the predator to its starting

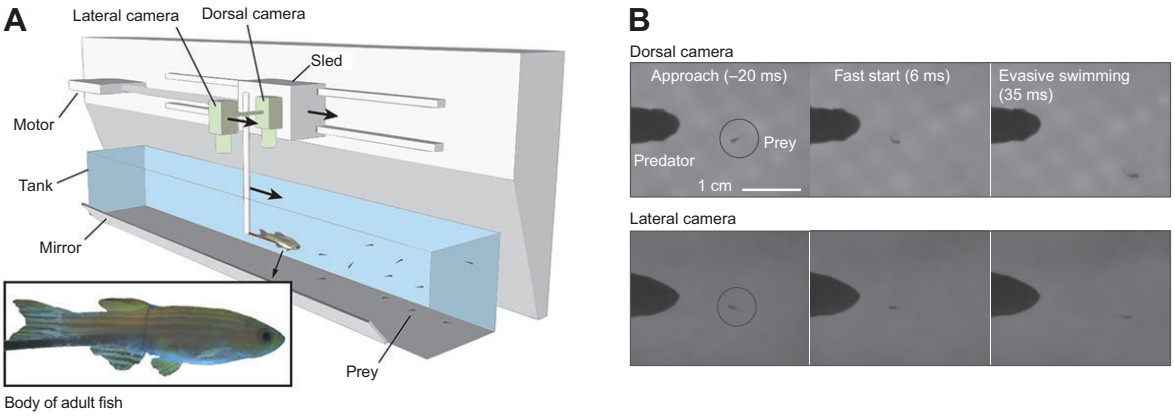

Fig. 9. The robotic predator used for behavioral experiments. (A) The tethered body of a dead adult fish was propelled through a water-filled tank to expose prey fish to the flow generated by a predator. The motor-driven sled that carried the predator provided a platform for two video cameras that monitored a volume of water anterior to the predator from dorsal and (using a mirror) lateral views. (B) A recording from these cameras in the dark (under IR illumination) from one experiment illustrates the 'fast-start' escape and subsequent swimming that prey exhibited in response to the robot's approach.

position, where it remained stationary for 5 min before another experiment commenced. Any prey within view of both the lateral and dorsal cameras was considered to be 'approached' by the predator. Preliminary experiments established that prey located outside the field of view of the cameras were positioned at least 1.25 cm away from the axis coincident with the predator midline and did not exhibit any response to the robot. To minimize repeated measures from the same larva, experiments on a group of prey ceased once the number of recorded escape responses tallied 15% of the total number of prey within the chamber. Prey responses were excluded if they occurred during the brief duration (<0.25 s) when the predator was changing speed at the start or end of translation. For this study, we included a total of 82, 80 and 76 recordings of prey that were respectively approached at 2, 11 and 20 cm s^{-1}.

We conducted an additional set of behavioral experiments to test the role of flow sensing in prey responses. This was achieved by compromising the lateral line in a group of larvae by exposure to a 250 µmol l^{-1} solution of neomycin sulphate for a 30 min period, followed by a 1 h recovery prior to experiments. This technique was developed in previous studies (Harris et al., 2003; McHenry et al., 2009), where it was shown to induce cell death in lateral line hair cells while leaving inner ear hair cells intact. In total, 200 prey with an ablated lateral line system were placed in the chamber for experiments, which resulted in 30 recordings of the robotic predator approaching treated prey.

We measured the location and direction of the fast start of larvae from our video recordings as a basis for determining the flow stimulus that triggers and directs this behavior. We used custom software developed in Matlab (v.2012b, with the image processing toolbox, MathWorks, Natick, MA, USA) to digitize three points along the prey body (rostrum tip, center of mass, tail tip) from both the dorsal and lateral images (Matlab datasets are available on request from M.J.M.). The body's center of mass was estimated as the midpoint between the prey's rostrum and the posterior margin of the swim bladder, which is consistent with prior work (Stewart and McHenry, 2010). A fast start was identified by the body rapidly (<15 ms) curling into a C shape, which is characteristic of stage 1 of this behavior (Weihs, 1972; Kimmel et al., 1974). We obtained body coordinates for the video frame prior to the initiation of stage 1 (i.e. the initial position). These coordinates were additionally recorded for the frame at which larvae completed stage 2 (when the body unfurls from a C shape) of the fast start, which was interpreted as the time at which the maneuver was completed. This frame was identified as when the tail reversed back to the direction of bending in stage 1. These landmark positions were transformed with respect to a coordinate system that was defined relative to the predator. Its origin was located at the anterior margin of the predator's rostrum, the x-axis was defined by the approach heading, and the z-axis as the opposite direction from gravity. Following the convention for a right-handed system, the y-axis coordinates were positive to the left of the predator and negative to the right. The response direction was characterized by the azimuth and elevation angles of the center of mass at the end of stage 2, relative to the initial position and accounting for the translation of the cameras. We verified that the direction established by the end of stage 2 was indicative of subsequent swimming in pilot experiments on 15 larvae where we recorded the direction of swimming over a wider field of view.

We scored the effectiveness of each fast start by whether it moved a larva away from the predator's heading. Responses directed 'away' from the predator occurred when the prey increased the distance separating the prey center of mass and the axis of the predator's heading between the start of the response and the end of stage 2. Conversely, responses were scored as being directed 'toward' the predator if the distance to the heading decreased during this time span. We additionally calculated the median values for azimuth and elevation, implemented the Circular Statistics Toolbox for Matlab (Berens, 2009). We also calculated the mean deviation, which is a metric of variation about a median value in circular statistics (Fisher, 1993).

We investigated whether the prey's position relative to the predator influenced the direction of a response. The elevation angles for responses were determined for prey that responded at positions dorsal to the heading axis of the predator (i.e. $z>0$) and those ventral to this axis (i.e. $z<0$). We considered the azimuth angles of responses by rectifying the y-values of response positions, which effectively created a mirror image of points that were to the right of the predator. We then divided these values by those that were lateral ($y>0.5$ cm) and medial (0 cm$<y<$0.5 cm) to the predator.

Computational fluid dynamics

We modeled the three-dimensional flow field around the body of our robotic predator with computational fluid dynamics (CFD) to investigate the flow that stimulates a directed fast start in prey. This model numerically solved the Navier–Stokes equations that govern fluid motion under boundary conditions for a Newtonian and incompressible fluid. These simulations were performed with a general-purpose commercial solver within ANSYS FLUENT (version 13.0.0; ANSYS Inc., Canonsburg, PA, USA) using the finite volume approach.

We measured the shape of the predator to define the boundaries of our fluid mesh. The surface of the predator was measured from digital photographs (1388×1040 pixels) of our preserved adult fish taken under a stereomicroscope (Zeiss Discovery V.20 and an AxioCam HRc camera, Carl Zeiss, Thornwood, NY, USA) from lateral and dorsal perspectives. Using custom software in Matlab, we traced the peripheral shape of the body to define the width and height of the body at 100 equally spaced positions along its length. We defined the volume of the body by approximating the transverse shape at each position with an ellipse of equivalent dimensions. The fins were excluded from our measurements and were thereby assumed to make a negligible contribution to the flow field.

The fluid volume surrounding the body (70×30×30 cm) was constructed using mesh generation software (GAMBIT, Lebanon, NH, USA). The surface of the predator was discretized into triangular meshes with ~0.4 mm edge lengths. The volume between the predator body surface and the surfaces of the fluid volume was discretized into tetrahedral control volumes. A no-slip boundary condition was prescribed at the body surface of the predator. A velocity-inlet boundary condition was prescribed at the surface facing the head of the predator fish and a pressure-outlet boundary condition was prescribed at the surface facing the tail of the predator. The remaining four outer boundary surfaces were prescribed with a symmetry boundary condition. The inlet velocity was set equal and opposite to the approach velocity for the same steady speeds used in our behavioral experiments (2, 11 and 20 cm s^{-1}). An additional series of simulations were conducted with zero viscosity to evaluate its influence on the predicted flow fields.

We analyzed the flow fields predicted by CFD to determine the flow around larvae at the time of their response. We accounted for the latency between a flow stimulus and escape response by calculating the 3D position of larvae relative to the predator 4 ms prior to the time at which we observed a response (Liu and Fetcho, 1999). However, a sensitivity analysis revealed that latencies of 0, 10 and 20 ms all yielded equal results. Using a Matlab script, we interpolated the flow velocities around the position at which each larva responded to the predator robot in our behavioral experiments (described above). In particular, we solved for velocity at 50 positions along the body, between our measured coordinates for the head and posterior margin of the tail. We additionally calculated the flows at 0.1 body lengths to the left, right, dorsal and ventral to the body along its length to determine the conditions around the body.

Flow visualization

We used the flow visualization technique of Particle Image Velocimetry (PIV) to test the predictions of our CFD model. PIV measurements were made by modifying the robotic predator setup used for our behavioral experiments (Fig. 10). The sled carrying the preserved predator also transported a single high-speed camera (Photron Fastcam 1024, Photron USA, San Diego, CA, USA) and the optics to project a sheet of laser light that illuminated particles suspended in the water around the predator. By this arrangement, the camera and light sheet translated in unison with the preserved predator to permit recordings of the motion of the particles around the predator's body. The video camera recorded at high resolution (1024×1024 pixels) and high speed (1000 frames s^{-1}) a 2.5 cm square region anterior and lateral to the predator's head using a macro lens (Nikkor 35–70mm, Nikon Corp., Tokyo, Japan). The laser beam (2 W, 532 nm wavelength, Laser Quantum, San Jose, CA, USA) was transmitted through a series of optics and mirrors to produce a horizontal light sheet that bisected

The Journal of Experimental Biology (2014) doi:10.1242/jeb.111773

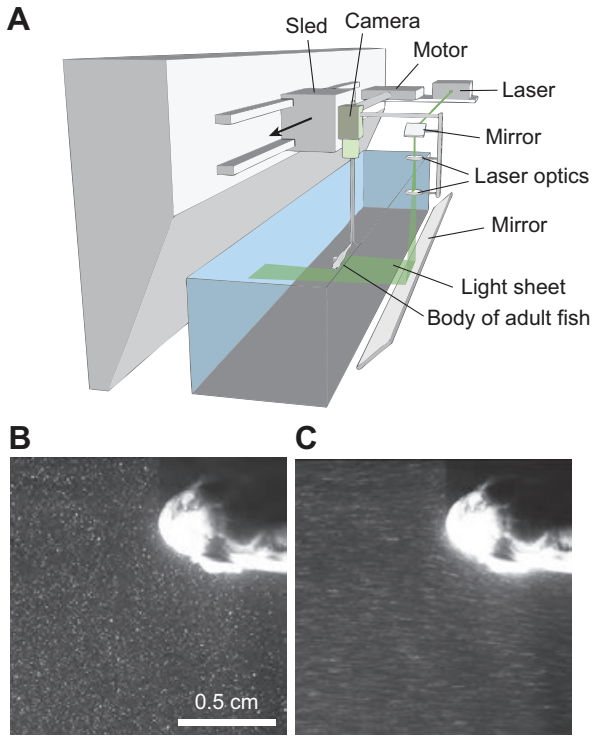

Fig. 10. Flow visualization by particle image velocimetry (PIV). (A) A schematic illustration of the modifications to our experimental setup (Fig. 9) for PIV recordings. This arrangement succeeded in translating a camera and laser sheet along with the preserved body of the predator to record the flow ahead of the predator's body. (B) A representative PIV image shows the illuminated particle field around the predator head. (C) Water flow around the predator moving with an approach speed of 2 cm s^{-1}. Particle streaks were generated by averaging 35 sequential video frames recorded at 1000 Hz.

the head of the predator. The particles illuminated by this light source consisted of reflective diamond powder (<1 µm diameter, Lasco Diamond Products, Inc., Chatsworth, CA, USA), dispersed at a density of 0.073 g l^{-1}. Video recordings were collected from dorsal and lateral perspectives of the predator by rotating its body around its longitudinal axis prior to recording. We performed these recordings for each of the approach speeds used in our behavioral experiments (2, 11 and 20 cm s^{-1}).

Software was used to calculate the velocity field from the video recordings. This software, OSIV (Open Source Image Velocimetry, osiv.sourceforge.net), used a fast, direct least-squares algorithm to track the two-dimensional displacement of particles between frames in a video recording. Each frame was divided into a 32×32 grid of cells (each cell had dimensions of 32×32 pixels), with the algorithm determining displacement for each cell to yield a regular grid for each pair of video frames. The corresponding velocity was calculated by multiplying displacements by the frame rate. After rejecting outliers, we found the mean value of the velocity of each cell over a recording of 200 frames. The software then offset the cells in both dimensions by 16 pixels and repeated the analysis in order to yield a 64×64 grid of vectors. We calculated flow in the global frame of reference by adding the approach velocity to all measured flow fields.

We compared the velocity fields calculated by PIV to the flow predicted by CFD using custom software within Matlab. This program interpolated the flow field predicted by CFD to determine the predicted flow velocity on the sagittal and frontal planes at the positions for which we measured flow by PIV. Differences between the PIV and CFD flow fields for the frontal and sagittal planes were quantified as the percentage difference in flow speed between corresponding locations. We found that the average difference between the PIV and CFD flow fields for all approach speeds was less than 7%. This suggests that our CFD simulations yielded a good approximation of the measured flow field around the robotic predator.

Behavioral algorithm modeling

We compared the fast-start direction expected for different behavioral algorithms. At each position and orientation for which we measured a response (Fig. 1A,B), we calculated a prediction for the azimuth of the fast-start direction using a Matlab script. Based on preliminary results, we modeled the flow reflex as a response that was directed normal to the initial orientation, away from the side of the body exposed to more rapid flow. Similarly, an algorithm modeled the response away from flow, but at a random angle with respect to the body. As a contrast, we modeled the responses predicted when directed toward the side of the body exposed to a faster flow velocity and responses that were entirely random. We tested whether the predictions of each algorithm were significantly different from our measurements using a non-parametric test known as a Kuiper test (Batschelet, 1981), as implemented in the Circular Statistics Toolbox for Matlab (Berens, 2009). This is analogous to a Kolmogorov–Smirnov test for circular statistics that also does not assume a particular distribution for the data. This appeared to be necessary when our preliminary analysis revealed that some of our measurements failed to conform to a von Mises distribution (Fisher, 1993).

Acknowledgements

We would like to thank K. Changsing for help with data analysis.

Competing interests

The authors declare no competing financial interests.

Author contributions

W.J.S. and M.J.M. designed the study, performed the major data analysis and wrote the manuscript. H.J. developed the CFD model and performed the simulations. A.N. performed the PIV analysis. All experiments were performed by W.J.S.

Funding

This work was supported by the National Science Foundation [grant numbers IOS-0952344 and IOS-1354842 to M.J.M.; OCE-1129496 to H.J.].

Supplementary material

Supplementary material available online at
http://jeb.biologists.org/lookup/suppl/doi:10.1242/jeb.111773/-/DC1

References

Batschelet, E. (1981). *Circular Statistics in Biology*. New York, NY: Academic Press.
Berens, P. (2009). CircStat: a MATLAB toolbox for circular statistics. *J. Stat. Softw.* **31**, 1-21.
Blaxter, J. H. S. and Fuiman, L. A. (1989). Function of the free neuromasts of marine teleost larvae. In *The Mechanosensory Lateral Line: Neurobiology and Evolution* (ed. S. Coombs, P. Görner and H. Münz), pp. 481-499. New York, NY: Springer-Verlag.
Brand, M., Granato, M., Nuesslein-Volhard, C., Nusslein-Volhard, C. and Dahm, R. (2002). Keeping and raising zebrafish. In *Zebrafish: A Practical Approach* (ed. C. Nusslein-Volhard and R. Dahm). Oxford: Oxford University Press.
Burgess, H. A. and Granato, M. (2007). Modulation of locomotor activity in larval zebrafish during light adaptation. *J. Exp. Biol.* **210**, 2526-2539.
Casas, J., Steinmann, T. and Dangles, O. (2008). The aerodynamic signature of running spiders. *PLoS ONE* **3**, e2116.
Day, S., Higham, T. and Wainwright, P. C. (2007). Time resolved measurements of the flow generated by suction feeding fish. *Exp. Fluids* **43**, 713-724.
Dijkgraaf, S. (1963). The functioning and significance of the lateral-line organs. *Biol. Rev. Camb. Philos. Soc.* **38**, 51-105.
Dill, L. (1974). Escape response of zebra danio (Brachydanio-rerio) 1. Stimulus for escape. *Anim. Behav.* **22**, 711-722.
Domenici, P., Blagburn, J. M. and Bacon, J. P. (2011). Animal escapology I: theoretical issues and emerging trends in escape trajectories. *J. Exp. Biol.* **214**, 2463-2473.
Dunnett, C. (1980). Pairwise multiple comparisons in the homogeneous variance, unequal sample size case. *J. Amer. Stat. Assoc.* **75**, 789-795.
Fisher, N. I. (1993). *Statistical Analysis of Circular Data*. Cambridge, UK: Cambridge University Press.
Fuiman, L. A. and Magurran, A. (1994). Development of predator defences in fishes. *Rev. Fish Biol. Fish.* **4**, 145-183.
Gemmell, B. J., Adhikari, D. and Longmire, E. K. (2014). Volumetric quantification of fluid flow reveals fish's use of hydrodynamic stealth to capture evasive prey. *J. R. Soc. Interface* **11**, 20130880.
Harris, J. A., Cheng, A. G., Cunningham, L. L., MacDonald, G., Raible, D. W. and Rubel, E. W. (2003). Neomycin-induced hair cell death and rapid regeneration in the lateral line of zebrafish (Danio rerio). *J. Assoc. Res. Otolaryngol.* **4**, 219-234.
Heuch, P. A., Doall, M. H. and Yen, J. (2007). Water flow around a fish mimic attracts a parasitic and deters a planktonic copepod. *J. Plankton Res.* **29**, i3-i16.

Holzman, R. and Wainwright, P. C. (2009). How to surprise a copepod: Strike kinematics reduce hydrodynamic disturbance and increase stealth of suction-feeding fish. *Limnol. Oceanogr.* **54**, 2201-2212.
Humphries, D. A. and Driver, P. M. (1970). Protean defence by prey animals. *Oecologia* **5**, 285-302.
Isaacs, R. (1965). *Differential Games: A Mathematical Theory with Applications to Warfare and Pursuit, Control and Optimization*. New York, NY: John Wiley & Sons, Inc.
Kimmel, C. B., Patterson, J. and Kimmel, R. O. (1974). The development and behavioral characteristics of the startle response in the zebra fish. *Dev. Psychobiol.* **7**, 47-60.
Kiørboe, T. and Visser, A. W. (1999). Predator and prey perception in copepods due to hydromechanical signals. *Mar. Ecol. Prog. Ser.* **179**, 81-95.
Liao, J. C. (2014). Functional architecture of lateral line afferent neurons in larval zebrafish. In *The Role of Flow and the Lateral Line in the Multisensory Guidance of Orienting Behaviors* (ed. H. Bleckmann, J. Mogdans and S. Coombs), pp. 319-332. Berlin: Springer-Verlag.
Liu, K. S. and Fetcho, J. R. (1999). Laser ablations reveal functional relationships of segmental hindbrain neurons in zebrafish. *Neuron* **23**, 325-335.
McHenry, M. J., Feitl, K. E., Strother, J. A. and Van Trump, W. J. (2009). Larval zebrafish rapidly sense the water flow of a predator's strike. *Biol. Lett.* **5**, 477-479.
Seamone, S., Blaine, T. and Higham, T. E. (2014). Sharks modulate their escape behavior in response to predator size, speed and approach orientation. *Zoology*. **117**, 377-382.
Stewart, W. J. and McHenry, M. J. (2010). Sensing the strike of a predator fish depends on the specific gravity of a prey fish. *J. Exp. Biol.* **213**, 3769-3777.
Stewart, W. J., Cardenas, G. S. and McHenry, M. J. (2013). Zebrafish larvae evade predators by sensing water flow. *J. Exp. Biol.* **216**, 388-398.
Viitasalo, M., Kiorboe, T., Flinkman, J., Pedersen, L. W. and Visser, A. W. (1998). Predation vulnerability of planktonic copepods: consequences of predator foraging strategies and prey sensory abilities. *Mar. Ecol. Prog. Ser.* **175**, 129-142.
Visser, A. W. (2001). Hydromechanical signals in the plankton. *Mar. Ecol. Prog. Ser.* **222**, 1-24.
Wainwright, P. C., Ferry-Graham, L. A., Waltzek, T. B., Carroll, A. M., Hulsey, C. D. and Grubich, J. R. (2001). Evaluating the use of ram and suction during prey capture by cichlid fishes. *J. Exp. Biol.* **204**, 3039-3051.
Weihs, D. (1972). A hydrodynamical analysis of fish turning manoeuvres. *Proc. R. Soc. B* **182**, 59-72.
Weihs, D. and Webb, P. (1984). Optimal avoidance and evasion tactics in predator-prey interactions. *J. Theor. Biol.* **106**, 189-206.
Westerfield, M. (1993). *The Zebrafish Book: A Guide for the Laboratory Use of Zebrafish (Brachydanio Rerio)*. Eugene, OR: University of Oregon Press.

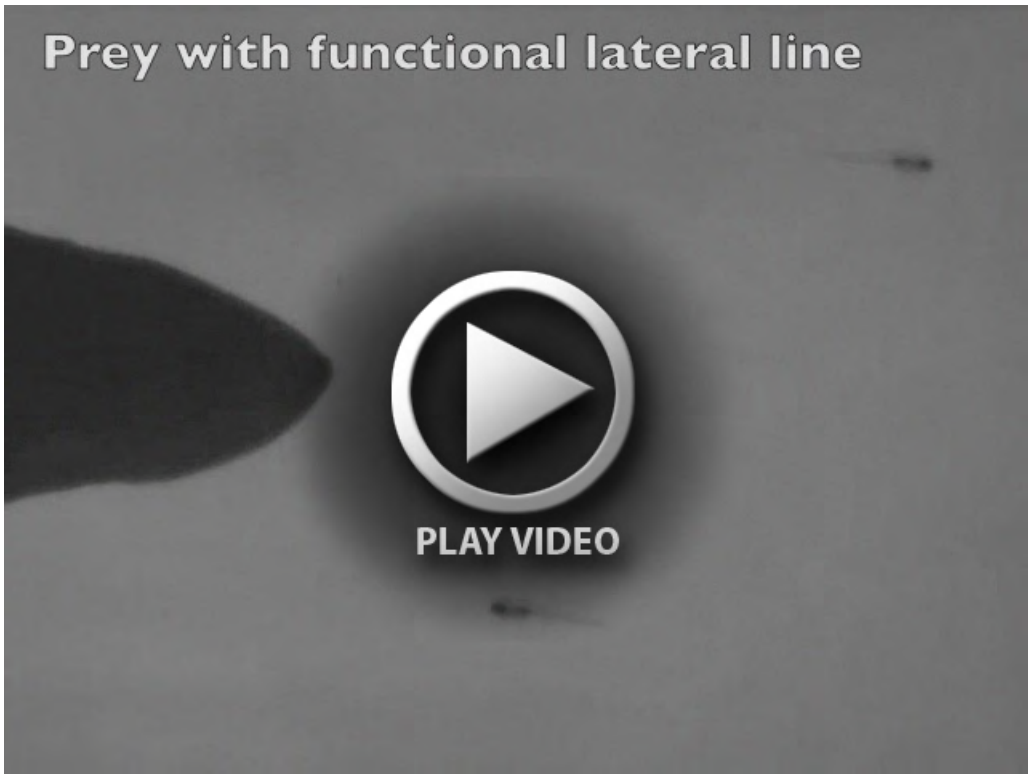

Movie 1. Responses of larvae with a functional lateral line system. A video recording from the lateral camera of our robotic predator (Fig. 1) recorded larvae in the dark, using IR illumination and an IR-sensitive camera. This recording shows representative 'fast start' responses of larvae to the robot.

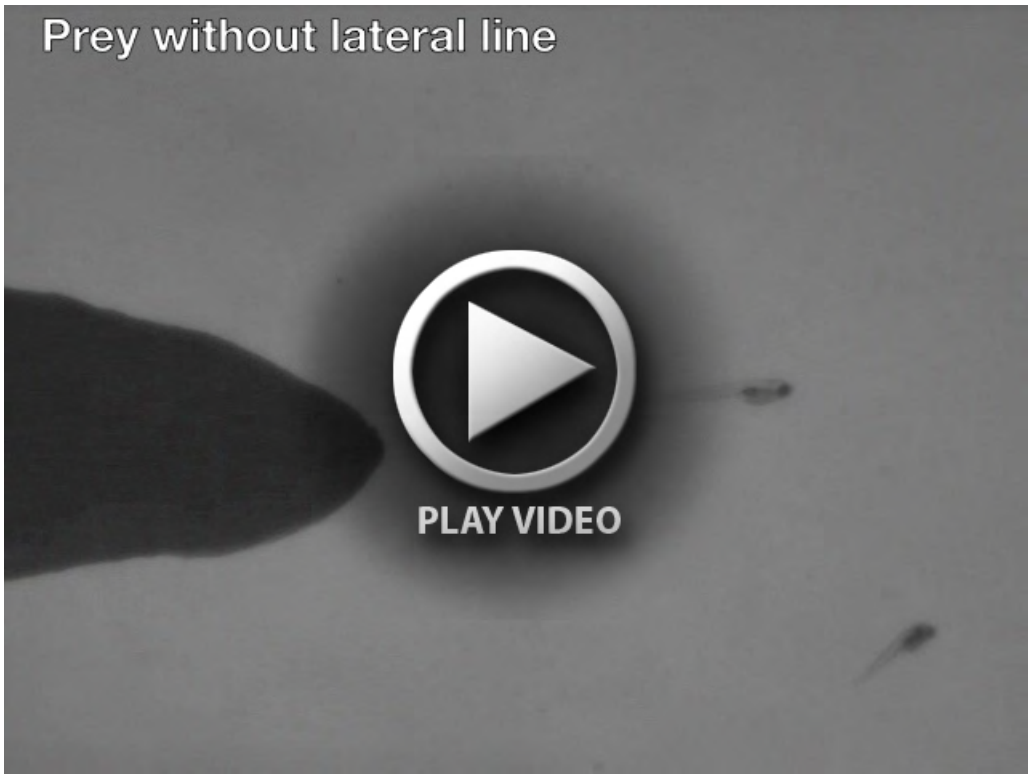

Movie 2. Responses of larvae without a functional lateral line system. As in Movie 1, we recorded the responses of larvae to the robot in the dark. However, in this experiment larvae were treated with an ototoxic antibiotic that compromised the functioning of the lateral line system. As a consequence, the larvae failed to sense the predator's approach and was consequently swept aside.